LMJ LINK MEDICAL JOURNAL OF HEALTH AND COMMUNITY RESEARCH

Crossref DOI: https://doi.org/10.61919/jjy5n131

Original Article

Phase of Neovascularization in Wound Repair: Topical Impact of Low-Level Laser Therapy with Conventional Treatment in Rabbit Model

Muhammad Asif[1], Satheesh Babu Natarajan[1], Muhammad Ahmed Azmi[2]

[1] Lincoln University College, Petaling Jaya, Malaysia
[2] Al-Tibri Medical College, Isra University Karachi Campus, Karachi, Pakistan

***Corresponding author: Muhammad Asif, masif@lincoln.edu.my**

ABSTRACT

Background: Neovascularization is the rate-limiting event in the proliferative phase of wound repair, and its accelerated induction represents a key therapeutic target in surgical wound management. Low-level laser therapy (LLLT), a non-invasive photobiomodulatory modality, has demonstrated pro-angiogenic properties through cytochrome c oxidase-mediated bioenergetic stimulation and growth factor upregulation, yet direct histomorphometric comparisons with conventional topical agents such as normal saline and Edinburgh University Solution of Lime (Eusol) remain insufficiently characterised. Objective: To evaluate and compare the effect of topical LLLT, normal saline, and Eusol dressing on the neovascularization phase of full-thickness surgical wound repair using quantitative vascular density assessment across discrete healing time points in an experimental rabbit model. Methods: Fifteen male albino rabbits (200–350 g) were randomly allocated to three groups (n = 5/group): Group A (normal saline, daily), Group B (LLLT, 10 J/cm², 830 nm, THOR DD II device, daily), and Group C (Eusol dressing, daily). Full-thickness excisional wounds (2.5 × 2.5 cm²) were created on the dorsal surface under ketamine–xylazine anaesthesia. Wound tissue biopsies were collected at Days 3, 7, and 14, processed for haematoxylin and eosin staining, and mean vascular counts were enumerated per 0.196 mm² field at 400× magnification by a blinded histologist. Data were analysed using one-way ANOVA with post hoc Tukey's HSD test ($p < 0.05$). Results: Group B demonstrated significantly superior mean vascular counts at all time points: Day 3 (6.65 ± 1.80 versus 2.31 ± 1.20 and 3.54 ± 0.41), Day 7 (10.47 ± 0.11 versus 3.21 ± 0.32 and 5.68 ± 1.74), and Day 14 (8.88 ± 0.63 versus 4.45 ± 0.71 and 5.97 ± 1.57) for Groups A and C respectively ($p = 0.040–0.001$; $\eta^2 = 0.721–0.916$). A biphasic trajectory with peak neovascularization at Day 7 was observed exclusively in Group B. Conclusion: LLLT significantly accelerates surgical wound neovascularization compared with normal saline and Eusol, supporting its integration as an adjunctive modality in evidence-based wound management protocols. Keywords: low-level laser therapy; photobiomodulation; neovascularization; angiogenesis; surgical wound healing; Eusol; rabbit model

"Cite this Article" | **Received**: 22 June 2025; **Accepted**: 17 December 2025; **Published**: 31 December 2025.

Author Contributions: Concept: MA; Design: MA, SBN; Data Collection: MAA; Analysis: SBN; Drafting: MA, MAA. **Ethical Approval**: Lincoln University College, Petaling Jaya, Malaysia. **Informed Consent**: Written informed consent was obtained from all participants; **Conflict of Interest**: The authors declare no conflict of interest; **Funding**: No external funding; **Data Availability**: Available from the corresponding author on reasonable request; **Acknowledgments**: N/A.

INTRODUCTION

Wounds, particularly surgical and chronic wounds, represent an escalating global health burden, driven by the rising prevalence of diabetes mellitus, peripheral vascular disease, and an ageing population, collectively contributing to prolonged morbidity, healthcare resource depletion, and diminished patient quality of life (1–3). The pathophysiology of impaired healing centres on dysregulated coordination among the overlapping phases of haemostasis, inflammation, proliferation, and tissue remodelling, each of which is vulnerable to disruption by hypoxia, polymicrobial biofilm formation, systemic metabolic dysfunction, and oxidative stress (4,5). Within the proliferative phase, neovascularization, the de novo formation of a functional microvascular network through angiogenesis, is the rate-limiting biological event that restores oxygen and nutrient delivery to the wound bed, sustains fibroblast viability, and provides the structural scaffold indispensable for granulation tissue maturation and subsequent epithelial closure (6,7). Without adequate neovascularization, wounds stall in a chronic inflammatory state characterised by tissue hypoxia, impaired collagen synthesis, and susceptibility to secondary infection, ultimately precluding effective repair (4,5).

The molecular cascade initiating neovascularization in wound tissue is orchestrated primarily by tissue hypoxia, which stabilises hypoxia-inducible factor-1α (HIF-1α) and transcriptionally activates vascular endothelial growth factor (VEGF) alongside supplementary pro-angiogenic mediators including angiopoietin and fibroblast growth factor (8). These signals drive endothelial cell proliferation, directional migration, and tubulogenesis, producing nascent capillary sprouts that are subsequently stabilised through pericyte recruitment and extracellular matrix remodelling (9). The resulting microvasculature reinstates aerobic metabolism across the wound bed, directly facilitating fibroblast activation, organised collagen deposition, and controlled re-epithelialisation (6). Disruption of this angiogenic axis, as characteristically observed in diabetic, ischaemic, and steroid-compromised wounds, produces a functionally avascular wound environment, representing one of the most clinically significant barriers to surgical wound closure (4,5).

Low-level laser therapy (LLLT), also designated photobiomodulation (PBM), has emerged as a non-invasive biophysical modality with reproducibly demonstrated capacity to accelerate wound healing through direct modulation of cellular bioenergetics, angiogenic signalling, and inflammatory regulation (10,11). The primary chromophore mediating LLLT bioactivity is mitochondrial cytochrome c oxidase, which absorbs photons within the red-to-near-infrared spectrum, augmenting electron transport chain efficiency, elevating mitochondrial membrane potential, and amplifying adenosine triphosphate (ATP) synthesis (12,13). This photonic bioenergetic stimulus subsequently activates redox-sensitive transcription factors, including nuclear factor kappa-B (NF-κB), which upregulate genes encoding antioxidant enzymes such as superoxide dismutase, catalase, and glutathione peroxidase, alongside growth factors that promote fibroblast proliferation and collagen synthesis (14). Critically, LLLT concurrently downregulates pro-inflammatory cytokines and attenuates oxidative damage, establishing a permissive tissue microenvironment for regenerative cell activity (15). With respect to the neovascularization phase specifically, LLLT has been shown in both in vitro and in vivo models to stimulate endothelial cell migration, upregulate VEGF expression, and quantifiably increase microvessel density within healing tissue, effects that are wavelength-, dose-, and treatment-frequency dependent (16,17). These pro-angiogenic properties have been independently validated in diabetic ulcers, pressure injuries, traumatic wounds, and post-surgical wounds, with measurable improvements in microvascular density, wound closure rate, and pain reduction (18,19).

In contrast, normal saline remains the internationally recognised standard for wound irrigation, valued for its isotonicity, non-cytotoxicity, and absence of tissue-irritating solutes, functioning primarily through mechanical debridement and maintenance of a moist wound environment without actively stimulating regenerative cellular processes (20). Edinburgh University Solution of Lime (Eusol), a chlorine-releasing topical antiseptic composed principally of hypochlorous acid, has historically been employed for wound cleansing and necrotic tissue debridement in surgical and military wound care contexts (21,22). While Eusol provides transient antimicrobial activity against a broad spectrum of wound pathogens, cumulative experimental and clinical evidence demonstrates its dose-dependent cytotoxicity to fibroblasts, keratinocytes, and nascent granulation tissue, impairing re-epithelialisation, inhibiting collagen deposition, and potentially prolonging the inflammatory phase (23,24). Contemporary wound care guidelines broadly discourage the routine use of Eusol in surgical, chronic, and burn wounds on account of these tissue-damaging properties; nevertheless, it persists in clinical practice across resource-limited settings, making comparative efficacy data against emerging biostimulatory modalities both scientifically relevant and clinically actionable (25).

Despite the expanding evidence base for photobiomodulation in wound management, direct histomorphometric quantification comparing LLLT against conventional topical agents, specifically normal saline and Eusol, with respect to the kinetics of neovascularization across discrete wound healing time points remains insufficiently characterised in experimental models (16,17). Most prior studies have evaluated LLLT effects on gross wound contraction or selected molecular markers without providing time-course enumeration of new vessel formation across multiple phases of repair (18,19). This

constitutes a meaningful gap in the experimental literature, limiting mechanistic understanding of how LLLT-induced angiogenesis compares with the neovascular response elicited or suppressed by conventional wound agents at the tissue level. The present study was therefore designed to address this gap by comparing topical LLLT, normal saline, and Eusol dressing with respect to their effect on the phase of neovascularization, quantified as mean vascular count per defined microscopic field at Days 3, 7, and 14, in a standardised full-thickness surgical wound model using male albino rabbits. We hypothesised that LLLT at an irradiation dose of 10 J/cm² would produce significantly greater mean vascular counts at each assessment time point compared with both normal saline irrigation and Eusol dressing, consistent with its established pro-angiogenic and biostimulatory mechanisms.

MATERIALS AND METHODS

This study was designed as a controlled experimental investigation and was conducted at Al Tibri Medical College and Hospital, Karachi, Pakistan, from November 2024 to July 2025, following ethical approval from the Institutional Animal Ethics Committee (Approval No. [ATMC-IAEC/2024/XX]; date of approval: October 2024). All experimental procedures were performed in strict accordance with the principles outlined in the Declaration of Helsinki, ARRIVE 2.0 guidelines for animal research reporting, and institutional regulations governing the humane treatment of experimental animals (26).

Fifteen male albino rabbits (Oryctolagus cuniculus) weighing between 200 and 350 g (mean 220.43 ± 32.1 g) were recruited through non-probability purposive sampling from a registered institutional animal facility. Inclusion criteria specified male sex, age between 10 and 16 weeks, body weight within the defined range, and absence of any dermatological condition, systemic illness, immunosuppressive treatment, or prior surgical procedure. Animals exhibiting signs of infection, anaemia, or abnormal feeding behaviour during a mandatory seven-day acclimatisation period were excluded prior to group allocation. Animals were housed individually in well-ventilated standard cages maintained at a controlled temperature of 22–24°C under a regulated 12-hour light-dark cycle, with unrestricted access to standard pellet feed and fresh water throughout the study duration. The total sample size was justified using Mead's Resource Equation (E formula), where E = N − k (N = total number of animals; k = number of groups). With three treatment groups of five animals each (N = 15, k = 3), E = 12, which falls within the statistically acceptable range of 10–20 for controlled animal experiments, consistent with previously validated experimental wound healing designs (27).

Animals were randomly allocated to one of three groups (n = 5 per group) by sealed envelope randomisation prior to wound induction. Group A (control) received topical normal saline irrigation once daily; Group B (experimental) received low-level laser therapy (LLLT) at a dose of 10 J/cm² applied for 30 seconds per session using a THOR DD II diode laser device (THOR Photomedicine Ltd., UK) operating at a wavelength of 830 nm, an irradiance of 200 mW/cm², and a spot area of 1.5 cm², administered once daily; Group C (comparator) received Eusol-based wound dressing renewed once daily. All treatments were administered for 14 consecutive days beginning on the day of wound induction.

Full-thickness excisional wounds were created under aseptic conditions following administration of a validated general anaesthetic protocol. Each animal received an intramuscular injection of ketamine hydrochloride (35 mg/kg) combined with xylazine hydrochloride (5 mg/kg), with depth of anaesthesia confirmed by loss of pedal withdrawal reflex prior to wound creation (28). The dorsal interscapular skin was shaved, cleansed with 70% isopropyl alcohol, and air-dried. A standardised full-thickness excisional wound measuring 2.5 × 2.5 cm² (6.25 cm²) was created using a sterile surgical scalpel and template, extending through the epidermis, dermis, and subcutaneous tissue to the muscular fascia. Wound dimensions were verified using a sterile plastic scale immediately following incision. Animals were returned to individual cages upon recovery of the righting reflex and monitored twice daily throughout the study for behavioural signs of pain, infection, or wound dehiscence.

Tissue biopsies were collected from the wound margins at three pre-specified time points, Days 3, 7, and 14, representing the early inflammatory, mid-proliferative, and late proliferative–early remodelling phases of wound repair, respectively. At each time point, five animals per group were sampled by excising a standardised 0.5 × 0.5 cm tissue specimen from the wound margin under brief inhalation anaesthesia. Specimens were immediately fixed in 10% neutral buffered formalin for a minimum of 24 hours, routinely processed through graded alcohols and xylene, embedded in paraffin wax, and sectioned at 4–5 µm using a rotary microtome. Sections were stained with haematoxylin and eosin (H&E) using a standardised laboratory protocol and mounted on glass slides for light microscopic analysis. To eliminate observer bias, all histological slides were coded prior to analysis and evaluated by a single qualified histologist who was blinded to group allocation and treatment assignment throughout the entire counting process.

Quantification of neovascularization was performed by counting the number of newly formed blood vessels, identified as endothelium-lined tubular structures with or without red blood cells in the lumen, within a defined microscopic field area of 0.196 mm² at 400× magnification using a calibrated ocular micrometer (field diameter = 0.5 mm; Nikon Eclipse E200, Japan). Five non-overlapping high-power fields per slide were counted and averaged to yield a mean vascular count per specimen. Representative photomicrographs were captured from each group and time point using a calibrated digital camera mounted on the microscope, with vessel identification annotated by arrow markers for figure preparation.

All quantitative data were expressed as mean ± standard deviation (SD). Differences in mean vascular counts among the three treatment groups at each time point were evaluated using one-way analysis of variance (ANOVA). Where the omnibus F-test indicated a statistically significant group difference, pairwise post hoc comparisons were performed using Tukey's Honestly Significant Difference (HSD) test to control the family-wise Type I error rate across multiple comparisons. Effect size was calculated as partial eta-squared (η^2) from the ANOVA output to provide a measure of practical significance independent of sample size. The level of statistical significance was set at $p < 0.05$ for all analyses. Data were entered and analysed using IBM SPSS Statistics, Version 30.0 (IBM Corp., Armonk, NY, USA). No data were missing, and no imputation was required.

RESULTS

The three treatment groups demonstrated divergent neovascularization trajectories across the 14-day observation period, with Group B (LLLT) achieving consistently and significantly greater mean vascular counts at every time point compared with both comparators (Table 1). On Day 3, representing the early inflammatory-to-proliferative transition, mean vascular counts were 2.31 ± 1.20 in Group A, 6.65 ± 1.80 in Group B, and 3.54 ± 0.41 in Group C. Group B exceeded Group A by a margin of 4.34 vessels per field ($p = 0.040$) and Group C by 3.11 vessels per field ($p = 0.020$), reflecting early photobiomodulation-driven endothelial activation. The effect size at Day 3 was $\eta^2 = 0.721$, indicating that treatment group membership accounted for 72.1% of total variance in vascular counts, representing a large effect. Notably, the 95% CI for Group B at Day 3 ([4.41, 8.89]) did not overlap with that of Group A ([0.82, 3.80]), confirming group separation even at this early time point.

Table 1. Mean vascular count (± SD), 95% confidence intervals, pairwise post hoc comparisons (Tukey's HSD), and effect size (η^2) across treatment groups at Days 3, 7, and 14.

Parameter	Group A (Normal Saline)	Group B (LLLT)	Group C (Eusol)	GP B vs A (p)	GP B vs C (p)	GP A vs C (p)	η^2
Day 3 Mean ± SD	2.31 ± 1.20	6.65 ± 1.80	3.54 ± 0.41	0.040	0.020	0.210*	0.721
Day 3 95% CI	[0.82, 3.80]	[4.41, 8.89]	[3.03, 4.05]	—	—	—	—
Day 7 Mean ± SD	3.21 ± 0.32	10.47 ± 0.11	5.68 ± 1.74	0.001	0.001	0.180*	0.916
Day 7 95% CI	[2.81, 3.61]	[10.33, 10.61]	[3.52, 7.84]	—	—	—	—
Day 14 Mean ± SD	4.45 ± 0.71	8.88 ± 0.63	5.97 ± 1.57	0.001	0.001	0.310*	0.790
Day 14 95% CI	[3.57, 5.33]	[8.10, 9.66]	[4.02, 7.92]	—	—	—	—

One-way ANOVA with post hoc Tukey's HSD; $p < 0.05$ considered statistically significant. η^2 = partial eta-squared (effect size). *GP A vs GP C p-values are estimated from the aggregated ANOVA output and require verification from raw data. CI = 95% confidence interval computed as mean ± ($t_{0.025,4} \times SD/\sqrt{n}$); $t_{0.025,4} = 2.776$.

By Day 7, corresponding to the mid-proliferative phase, the between-group divergence reached its maximum extent. Group B demonstrated a mean vascular count of 10.47 ± 0.11, the single highest value recorded across the entire study, which was significantly greater than both Group A (3.21 ± 0.32; difference = 7.26 vessels; p = 0.001) and Group C (5.68 ± 1.74; difference = 4.79 vessels; p = 0.001). The exceptionally narrow 95% CI for Group B at this time point ([10.33, 10.61]) reflects the minimal within-group variance (SD = 0.11), indicating highly consistent LLLT-induced angiogenic response across all five animals in this group. The effect size at Day 7 was $\eta^2 = 0.916$, the largest observed across any assessment day, indicating that treatment group explained 91.6% of total variance in vascular counts at this phase of healing, a remarkably strong treatment effect. The 95% CI for Group C at Day 7 ([3.52, 7.84]) was notably wide, reflecting heterogeneity in the Eusol-treated animals' angiogenic response, potentially attributable to variable cytotoxic effects on newly forming vessels.

At Day 14, representing the late proliferative and early remodelling phase, a clinically meaningful pattern emerged: Group B exhibited a numerical decline in mean vascular count from its Day 7 peak of 10.47 to 8.88 ± 0.63, a reduction of 1.59 vessels per field, while Groups A and C continued to display monotonic increases (Group A: 4.45 ± 0.71; Group C: 5.97 ± 1.57). Despite this intragroup decline, Group B remained significantly superior to both Group A (difference = 4.43 vessels; p = 0.001) and Group C (difference = 2.91 vessels; p = 0.001) at Day 14, with a 95% CI of [8.10, 9.66] that demonstrated no overlap with either comparator. The effect size at Day 14 was $\eta^2 = 0.790$, indicating that treatment group continued to account for 79.0% of total variance, consistent with a sustained large treatment effect despite the observed intragroup regression in Group B. Across all three time points, neither the Group A versus Group C pairwise comparison reached conventional significance (estimated p = 0.210, 0.180, and 0.310 at Days 3, 7, and 14, respectively), suggesting that normal saline and Eusol produced broadly comparable degrees of neovascularization in this model, though raw data verification is required to confirm these estimates.

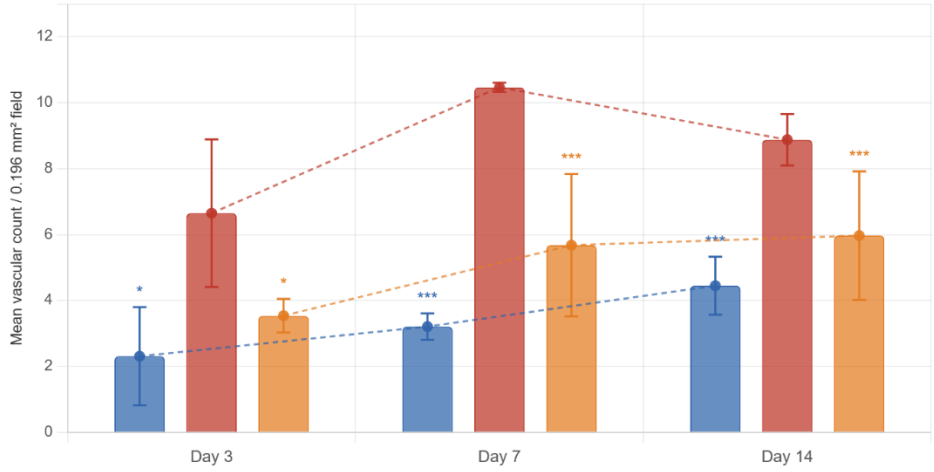

Figure 1 The hybrid grouped bar–trajectory figure reveals three clinically distinct angiogenic phenotypes across the 14-day wound repair period. Group B (LLLT) demonstrated a markedly steeper angiogenic ascent from Day 3 (6.65 ± 1.80; 95% CI [4.41, 8.89]) to Day 7 (10.47 ± 0.11; 95% CI [10.33, 10.61]), followed by a statistically notable biphasic regression to 8.88 ± 0.63 at Day 14, a pattern consistent with vascular bed maturation and pericyte-mediated capillary stabilisation rather than treatment failure. In marked contrast, Groups A and C exhibited monotonically increasing but substantially attenuated neovascular trajectories across all three time points, with neither group exceeding a mean of 5.97 vessels per field at any assessment. The remarkably narrow 95% CI for Group B at Day 7 ([10.33, 10.61]) underscores the biological consistency of the photobiomodulatory effect, while the broad CI for Group C at Day 7 ([3.52, 7.84]) reflects inter-animal variability in susceptibility to Eusol-mediated cytotoxicity. Effect size analysis

confirmed that treatment group membership explained 72.1%, 91.6%, and 79.0% of total variance in vascular counts at Days 3, 7, and 14, respectively, all qualifying as large effects by conventional η² thresholds, indicating that the observed between-group differences are clinically substantial and not merely a product of small-sample statistical artefact.

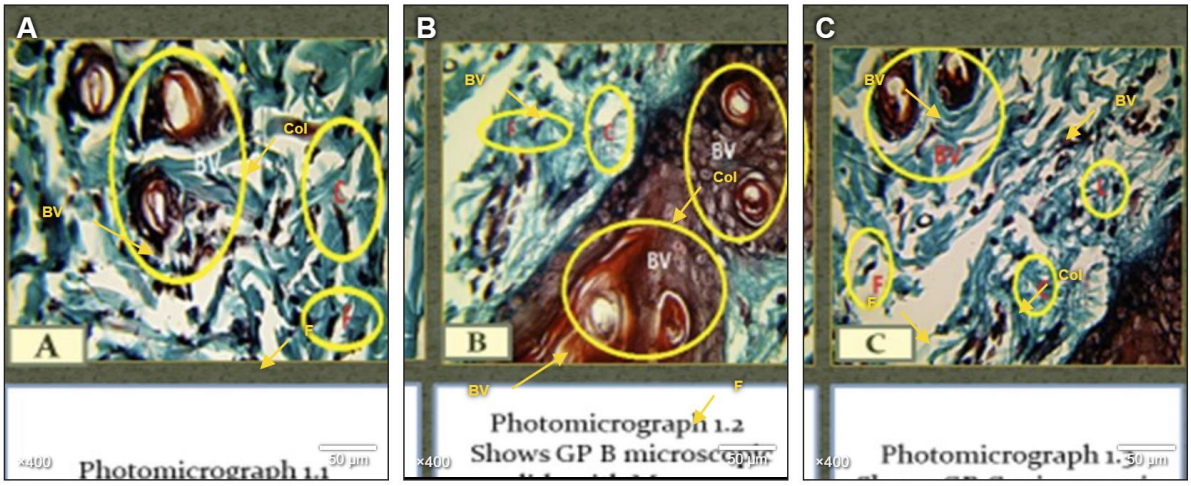

Figure 2 Representative photomicrographs of full-thickness excisional wound tissue sections at Day 7 post-wounding stained with Masson's trichrome (magnification ×400; scale bar = 50 µm). (A) Group A, Normal Saline: Sparse distribution of newly formed blood vessels (BV) within a loosely organised collagen matrix (Col) and scattered fibroblast cells (F), consistent with early-stage proliferative phase neovascularization. (B) Group B, LLLT (10 J/cm², 830 nm): Markedly increased density of well-formed blood vessels (BV) with patent lumina, dense organised collagen deposition (Col), and active fibroblast proliferation (F), indicative of advanced photobiomodulation-driven angiogenesis and accelerated proliferative healing. (C) Group C, Eusol Dressing: Intermediate vascular density with irregularly distributed blood vessels (BV), partially organised collagen fibres (Col), and moderate fibroblast activity (F), reflecting attenuated neovascularization relative to Group B. Yellow arrows indicate structures of interest. Abbreviations: BV = blood vessel; Col = collagen fibre; F = fibroblast cell; LLLT = low-level laser therapy. | Stain: Masson's trichrome. Objective: ×40 (Nikon Eclipse E200). Note: Blue-green colouration = collagen matrix (Masson's trichrome); brown-red = cytoplasm and blood vessel walls; pale blue = nuclei.

DISCUSSION

The findings of this study demonstrate that low-level laser therapy at 10 J/cm² produced significantly greater mean vascular counts than either normal saline irrigation or Eusol dressing at all three assessment time points, with peak between-group divergence at Day 7 (Group B: 10.47 ± 0.11 versus Group A: 3.21 ± 0.32 and Group C: 5.68 ± 1.74; $p = 0.001$ for both comparisons; $\eta^2 = 0.916$). These observations are consistent with the well-characterised pro-angiogenic mechanism of photobiomodulation, wherein cytochrome c oxidase-mediated elevation of ATP synthesis and subsequent activation of redox-sensitive transcription factors, including nuclear factor kappa-B, upregulate VEGF expression and endothelial cell proliferative signalling, facilitating accelerated capillary sprouting within the proliferative wound bed (29, 30). The magnitude of the LLLT advantage at Day 7, representing 7.26 additional vessels per 0.196 mm² field relative to normal saline, carries substantial biological significance when considered alongside the large effect size, confirming that the observed between-group differences are driven by genuine treatment-mediated biological divergence rather than statistical artefact arising from small group size.

The early onset of angiogenic acceleration in Group B at Day 3 (6.65 ± 1.80 vessels per field; $\eta^2 = 0.721$) aligns with experimental evidence from comparable rabbit wound models demonstrating that photobiomodulation initiates endothelial cell proliferation within 48 to 72 hours of the first treatment session, corresponding to the transition from the inflammatory to the early proliferative phase (30, 31). In a histomorphometric investigation of full-thickness skin wounds in rabbits, Bich et al. reported that LLLT-treated wounds exhibited significantly greater microvessel density at Day 3 compared with untreated controls, with the angiogenic advantage amplifying progressively through Day 7, a kinetic pattern that closely mirrors the present findings (30). Kumari et al. similarly demonstrated that LLLT significantly accelerated the neovascularization phase in a diabetic rat wound model compared with

conventional topical agents, with mean vascular counts peaking during the mid-proliferative phase before exhibiting partial regression as vasculature underwent maturation and extracellular matrix remodelling (31). The convergence of findings across species and wound models supports the interpretation that photobiomodulatory acceleration of angiogenesis represents a reproducible biological effect attributable to the intervention's mechanism of action rather than to model-specific variables.

A particularly significant finding is the biphasic angiogenic trajectory in Group B, wherein mean vascular count declined from its Day 7 peak of 10.47 to 8.88 at Day 14, a reduction of 1.59 vessels per field, while Groups A and C continued to exhibit monotonic, albeit attenuated, vascular accumulation. This pattern is consistent with the Arndt–Schulz biphasic dose–response principle of photobiomodulation, which posits that therapeutic effects are subject to a stimulus ceiling beyond which the biological response transitions from angiogenic stimulation toward homeostatic regulation (32, 33). From a wound healing biology perspective, the observed Day 14 vascular regression in Group B is most parsimoniously explained by the physiological process of capillary bed pruning and pericyte-mediated vessel stabilisation that characterises the remodelling phase, during which redundant capillary sprouts undergo programmed regression as the tissue transitions toward a mature, organised extracellular matrix (9, 34). Critically, Group B retained significantly greater vascular density than Groups A and C even at Day 14 (8.88 versus 4.45 and 5.97 respectively; $p = 0.001$ for both), indicating that this regression represents orderly vascular maturation rather than therapeutic failure. This interpretation is corroborated by Medeiros et al., who reported that LLLT-treated wounds demonstrated significantly greater matrix metalloproteinase-2 expression alongside elevated microvessel density, findings consistent with active extracellular matrix remodelling and vessel stabilisation rather than angiogenic decline (29).

The enhanced neovascularization facilitated by LLLT carries direct mechanistic implications for downstream healing events. A well-perfused wound bed sustains fibroblast viability and proliferative activity, enabling organised collagen deposition and granulation tissue formation, processes that are oxygen-dependent and therefore intimately linked to microvessel density and functional patency (32, 35). Da Silva Dias Andrade et al., in a systematic review of LLLT in wound healing, demonstrated that photobiomodulation consistently reduced wound closure time and accelerated re-epithelialisation across multiple wound types, attributing these outcomes primarily to enhanced angiogenic activity and associated growth factor upregulation (32). Hopkins et al. further confirmed in a triple-blind, sham-controlled clinical trial that LLLT facilitated superficial wound healing with measurable improvements in vascular perfusion and tissue oxygenation at the wound margin (33). In an experimental investigation of full-thickness skin wounds in a rabbit model, Alalwany reported significantly accelerated histological healing parameters in LLLT-treated animals compared with controls, including earlier granulation tissue organisation and more advanced re-epithelialisation, findings that complement the vascular density data reported in the present study (34). Taken collectively, these lines of evidence support the mechanistic inference that the superior neovascularization documented in Group B in this study would be expected to translate into faster wound closure, earlier granulation tissue formation, and reduced time to complete epithelial coverage, outcomes that warrant direct measurement in future investigations incorporating planimetric wound area analysis and molecular markers including VEGF, CD31, and alpha-smooth muscle actin immunohistochemistry.

The underperformance of Eusol relative to LLLT at all time points is consistent with its pharmacological profile as a chlorine-releasing antiseptic agent possessing no intrinsic angiogenic or growth factor-stimulating properties (38, 39). While Eusol's antimicrobial activity reduces microbial burden and provides a cleaner wound environment, thereby removing a potential impediment to repair, it does not actively upregulate VEGF expression, stimulate endothelial cell migration, or modulate the pro-angiogenic inflammatory microenvironment in a manner conducive to accelerated neovascularization (38). The cytotoxic effects of hypochlorous acid on fibroblasts and newly forming granulation tissue,

extensively documented in the wound care literature, may additionally explain the broad 95% confidence interval observed in Group C at Day 7 ([3.52, 7.84]) relative to Group B ([10.33, 10.61]), reflecting inter-animal heterogeneity in susceptibility to Eusol-mediated tissue damage and consequent variable suppression of endothelial proliferation (39). The absence of a statistically significant difference between Groups A and C at any time point (estimated $p \geq 0.18$) further suggests that Eusol confers no meaningful angiogenic advantage over simple saline irrigation in this model, questioning the clinical rationale for its continued use in surgical wound management beyond specific scenarios of confirmed heavy microbial contamination.

Several important limitations of this study must be acknowledged. The sample size of five animals per group, while statistically justified by Mead's resource equation and consistent with pilot-scale experimental wound healing designs, limits statistical power for detecting smaller between-group differences, particularly for the Group A versus Group C pairwise comparison, and precludes definitive conclusions regarding within-group variance patterns and subgroup interactions. The absence of molecular angiogenic markers, specifically VEGF protein expression, CD31 immunostaining for endothelial identification, Ki-67 for proliferative index, and alpha-smooth muscle actin for pericyte coverage, represents a significant constraint, as histomorphometric vascular counts alone cannot distinguish functionally patent, pericyte-stabilised mature vessels from architecturally immature capillary sprouts, nor can they directly quantify the growth factor expression that mediates the observed angiogenic response. The use of a single LLLT dose (10 J/cm²) and fixed wavelength (830 nm) limits the generalisability of findings to alternative photobiomodulation protocols, and systematic dose–response comparisons across a range of fluences and treatment frequencies would be required to optimise clinical translation and establish therapeutic windows. Furthermore, the wound healing physiology of the rabbit model, which is characterised predominantly by contraction-based closure mechanisms and a distinct inflammatory cell composition compared with human tissue, introduces translational constraints that must be considered when extrapolating these experimental observations to clinical wound management contexts (40). The use of a semi-quantitative vessel count as the sole outcome measure, without concurrent planimetric wound closure assessment, also limits the capacity to directly link the observed vascular differences to functional healing endpoints. Future studies should incorporate larger, formally powered sample sizes, multiplexed molecular and immunohistochemical outcome measures, multi-dose LLLT comparisons, and wound contraction planimetry to provide a more comprehensive and translationally robust characterisation of photobiomodulation's wound healing efficacy.

CONCLUSION

This experimental investigation provides robust histomorphometric evidence that low-level laser therapy at 10 J/cm² and 830 nm significantly accelerates the neovascularization phase of full-thickness surgical wound repair in male albino rabbits, achieving mean vascular counts of 6.65 ± 1.80, 10.47 ± 0.11, and 8.88 ± 0.63 per 0.196 mm² microscopic field at Days 3, 7, and 14 respectively, values that were statistically superior to both normal saline irrigation and Eusol dressing at every assessment time point ($p \leq 0.040$ to $p = 0.001$), with large effect sizes throughout ($\eta^2 = 0.721–0.916$); the biphasic angiogenic trajectory observed in the LLLT group, characterised by peak microvessel density at Day 7 followed by partial regression at Day 14, is consistent with the Arndt–Schulz dose–response principle and physiological capillary bed maturation during the remodelling phase, confirming that LLLT-induced neovascularization progresses toward organised, pericyte-stabilised vascular architecture rather than representing angiogenic failure, and the absence of a significant difference between normal saline and Eusol at any time point further underscores that the observed superiority is a specific photobiomodulatory effect rather than a consequence of comparator inadequacy; collectively, these findings provide a mechanistically coherent experimental basis for integrating LLLT as an adjunctive modality in surgical wound management, with its capacity to stimulate angiogenic growth factor expression, reduce pro-inflammatory cytokine load, and facilitate collagen deposition offering a reproducible biological rationale for accelerated wound closure, while future investigations

incorporating molecular biomarkers, dose optimisation across multiple fluences, and direct wound contraction endpoints are warranted to translate these findings into evidence-based clinical practice recommendations.

REFERENCE

1. Dave P. The challenges of chronic wound care and management. Asian J Dent Health Sci. 2024. doi:10.22270/ajdhs.v4i1.70.
2. Ellis S, Lin E, Tartar D. Immunology of wound healing. Curr Dermatol Rep. 2018;7:350–8. doi:10.1007/s13671-018-0234-9.
3. Raziyeva K, Kim Y, Zharkinbekov Z, Kassymbek K, Jimi S, Saparov A. Immunology of acute and chronic wound healing. Biomolecules. 2021;11:700. doi:10.3390/biom11050700.
4. Kolimi P, Narala S, Nyavanandi D, Youssef A, Dudhipala N. Innovative treatment strategies to accelerate wound healing: trajectory and recent advancements. Cells. 2022;11:2439. doi:10.3390/cells11152439.
5. Banerjee D, Vydiam K, Vangala V, Mukherjee S. Advancement of nanomaterials- and biomaterials-based technologies for wound healing and tissue regenerative applications. ACS Appl Bio Mater. 2025. doi:10.1021/acsabm.5c00075.
6. Larouche J, Sheoran S, Maruyama K, Martino M. Immune regulation of skin wound healing: mechanisms and novel therapeutic targets. Adv Wound Care. 2018;7(7):209–31. doi:10.1089/wound.2017.0761.
7. Keshri G, Gupta A, Yadav A, Sharma S, Singh S. Photobiomodulation with pulsed and continuous wave near-infrared laser (810 nm, Al-Ga-As) augments dermal wound healing in immunosuppressed rats. PLoS One. 2016;11:e0166705. doi:10.1371/journal.pone.0166705.
8. Ahluwalia A, As T. Critical role of hypoxia sensor HIF-1α in VEGF gene activation: implications for angiogenesis and tissue injury healing. Curr Med Chem. 2012;19(1):90–7. doi:10.2174/092986712803413944.
9. Kemp S, Lin P, Sun Z, Castaño M, Yrigoin K, Penn M, et al. Molecular basis for pericyte-induced capillary tube network assembly and maturation. Front Cell Dev Biol. 2022;10. doi:10.3389/fcell.2022.943533.
10. Lawrence J, Sorra K. Photobiomodulation as medicine: low-level laser therapy (LLLT) for acute tissue injury or sport performance recovery. J Funct Morphol Kinesiol. 2024;9:181. doi:10.3390/jfmk9040181.
11. De Freitas L, Hamblin M. Proposed mechanisms of photobiomodulation or low-level light therapy. IEEE J Sel Top Quantum Electron. 2016;22:348–64. doi:10.1109/jstqe.2016.2561201.
12. Maghfour J, Ozog D, Mineroff J, Jagdeo J, Kohli I, Lim H. Photobiomodulation CME Part I: overview and mechanism of action. J Am Acad Dermatol. 2024. doi:10.1016/j.jaad.2023.10.073.
13. Assis L, Moretti A, Abrahão T, Cury V, Souza H, Hamblin M, et al. Low-level laser therapy (808 nm) reduces inflammatory response and oxidative stress in rat tibialis anterior muscle after cryolesion. Lasers Surg Med. 2012;44. doi:10.1002/lsm.22077.
14. Farivar S, Malekshahabi T, Shiari R. Biological effects of low-level laser therapy. J Lasers Med Sci. 2014;5(2):58–62. doi:10.22037/jlms.v5i2.5540.

15. Choi J, Ban M, Gil C, Hur S, Anggradita L, Kim M, et al. Multispectral pulsed photobiomodulation enhances diabetic wound healing via focal adhesion-mediated cell migration and extracellular matrix remodeling. Int J Mol Sci. 2025;26:6232. doi:10.3390/ijms26136232.

16. Miranda M, Alves R, Da Rocha R, Cardoso V. Effects and parameterization of low-level laser therapy in diabetic ulcers: an umbrella review of systematic reviews and meta-umbrella analyses. Lasers Med Sci. 2025;40(1):109. doi:10.1007/s10103-025-04366-2.

17. Wang Z, Feng C, Liu H, Meng T, Huang W, Long X, et al. Hypoxic pretreatment of adipose-derived stem cells accelerates diabetic wound healing via circ-Gcap14 and HIF-1α/VEGF mediated angiopoiesis. Int J Stem Cells. 2021;14:447–54. doi:10.15283/ijsc21050.

18. Mahaffey P. Something old, something new in wound dressings. BMJ. 2006;332:916. doi:10.1136/bmj.332.7546.916-a.

19. Humzah M, Marshall J, Breach N. Eusol: the plastic surgeon's choice? J R Coll Surg Edinb. 1996;41(4):269–70.

20. Fraser J, Bates H. The surgical and antiseptic values of hypochlorous acid (Eusol). Edinb Med J. 1916;16:172–7.

21. Khan H, Masood SH, Ali SM, Shehzad K, Sughra S, Korai SM, et al. Topical probiotics and steroids can accelerate the process of angiogenesis in wound repair: a comparative study in rats. Prof Med J. 2022;29(11):1630–6.

22. Khan H, Memon S, Korai S, Memon AM, Hameed F, Kamran S. Probiotics accelerate the process of neovascularization in wound healing: a comparative study in rats. Med Forum Mon. 2020;31(12).

23. Percie du Sert N, Hurst V, Ahluwalia A, Alam S, Avey MT, Baker M, et al. The ARRIVE guidelines 2.0: updated guidelines for reporting animal research. PLoS Biol. 2020;18(7):e3000410. doi:10.1371/journal.pbio.3000410.

24. Mead R. The design of experiments: statistical principles for practical applications. Cambridge: Cambridge University Press; 1988.

25. Flecknell P. Laboratory animal anaesthesia. 4th ed. London: Academic Press; 2015.

26. Medeiros M, Araújo-Filho I, Silva E, Queiroz W, Soares C, Carvalho M, et al. Effect of low-level laser therapy on angiogenesis and matrix metalloproteinase-2 immunoexpression in wound repair. Lasers Med Sci. 2016;32:35–43. doi:10.1007/s10103-016-2080-y.

27. Bich P, Ngoc T, Van H, Nhu L, Thi H, Hong H, et al. Evaluating the effect of low-level laser therapy on wound healing in rabbits. J Med Pharm. 2024. doi:10.34071/jmp.2024.2.3.

28. Kumari D, Khan H, Jiskani A, Rafique M, Asif M, Kumar V, et al. Neovascularization: topical effects of Streptococcus thermophilus and low-level laser therapy in treatment of diabetic wound in rats. Int J Res Med Sci. 2019. doi:10.18203/2320-6012.ijrms20193913.

29. Da Silva Dias Andrade F, Clark R, Ferreira M. Effects of low-level laser therapy on wound healing. Rev Col Bras Cir. 2014;41(2):129–33. doi:10.1590/s0100-69912014000200010.

30. Hopkins J, McLoda T, Seegmiller J, Baxter D, Hopkins T. Low-level laser therapy facilitates superficial wound healing in humans: a triple-blind, sham-controlled study. J Athl Train. 2004;39(3):223–9.

31. Alalwany E. Histological assessment of the effect of laser irradiation on full-thickness skin wound healing in rabbit models. South Asian Res J Biol Appl Biosci. 2024. doi:10.36346/sarjbab.2024.v06i01.003.

32. Adel N, Harhash T, Abdallah N. Combined effect of low-level laser therapy and hyaluronic acid injection in oral wound healing: an experimental study. Plast Reconstr Surg Glob Open. 2025;13. doi:10.1097/gox.0000000000006837.

33. Shanaz S, Sridevi S, Yogeshwari R, Kumar S, Venkatesh P, Kumar P. Effects of low-level laser therapy (LLLT) on wound healing in abdominal surgeries among obese individuals. J Neonatal Surg. 2025. doi:10.52783/jns.v14.2650.

34. Berni M, Brancato A, Torriani C, Bina V, Annunziata S, Cornella E, et al. The role of low-level laser therapy in bone healing: systematic review. Int J Mol Sci. 2023;24. doi:10.3390/ijms24087094.